Soil Dynamics and Earthquake Engineering 113 (2018) 202–214

Contents lists available at ScienceDirect

Soil Dynamics and Earthquake Engineering

journal homepage: www.elsevier.com/locate/soildyn

Assessment of the cyclic strain approach for evaluating liquefaction triggering

E. Rodriguez-Arriaga, R.A. Green*

Department of Civil and Environmental Engineering, Virginia Tech, Blacksburg, VA, USA

ARTICLE INFO

Keywords:
Liquefaction
Liquefaction Triggering
Cyclic Strain Approach
Cyclic Stress Approach
Dobry et al. (1982)

ABSTRACT

The cyclic strain approach was proposed in the 1980s as a potential alternative to the stress-based simplified liquefaction evaluation procedure. However, despite its fundamental basis and many positive attributes, it has not been embraced by practice. One reason for this may be the need to perform cyclic laboratory tests on undisturbed/reconstituted samples to develop a relationship among excess pore water pressure, cyclic strain amplitude, and number of applied strain cycles. Herein an alternative implementation of the strain-based procedure is proposed that circumvents this requirement, using a strain-based pore pressure generation model in lieu of laboratory test data. To assess the efficacy of the alternative implementation, several hundred small strain shear wave velocity (V_s) and Standard Penetration Test (SPT) field liquefaction case histories are evaluated. The results are compared with both field observations and with predictions from the stress-based procedures. It was found that the stress-based approach yielded considerably more accurate predictions compared to the cyclic strain approach. One likely reason for this is the strain-based procedure's inherent and potentially fatal limitation of ignoring the decrease in soil stiffness due to excess pore pressure when representing the earthquake loading in terms of shear strain amplitude and number of equivalent cycles.

1. Introduction

The primary objective of the study presented herein is to evaluate the efficacy of the strain-based liquefaction triggering evaluation procedure implemented using a pragmatic variant of the procedure originally proposed by Dobry et al. [11]. Liquefaction is a phenomenon that results from the contractive tendencies of loose to medium dense soils when sheared. For saturated cohesionless soils, this tendency results in the transfer of the overburden stress to the pore fluid, with the commensurate increase in pore water pressure and decrease in effective confining stress. Liquefaction has occurred in most major earthquakes and has caused significant damage to infrastructure (e.g., Cubrinovski and Green [8]; Cubrinovski et al. [9]; Green et al. [15]; Olson et al. [33]; Stringer et al. [40]; among many others).

The most widely used procedure for evaluating liquefaction triggering potential is the simplified stress-based procedure originally proposed by Whitman [44] and Seed and Idriss [37]. This procedure is semi-empirical and has undergone periodic updates as a result of findings from new laboratory studies and/or the collection and analysis of additional field case history data (e.g., Youd et al. [46]; Cetin et al. [6]; Idriss and Boulanger [16]). Inherent to this procedure is the quantification of the seismic demand imposed on the soil expressed in terms of cyclic shear stress.

Despite the popularity of the stress-based procedures, multiple studies have shown that excess pore water pressure better correlates to cyclic strain than to cyclic stress (e.g., Fig. 1) (e.g., Martin et al. [25]; Dobry et al., [11]; Byrne [3]). The reason for this is the relative movement of soil particles, which is requisite for excess pore water pressure generation, relates to the induced strain, regardless of amplitude of the stress applied to soil. As a result, Dobry et al. [11] proposed a strain-based liquefaction triggering evaluation procedure. Although the Dobry et al. [11] procedure generally received a positive reception by liquefaction researchers, it has failed to be adopted into practice. One reason for this is likely the requirement to perform strain-controlled cyclic laboratory tests on undisturbed and/or reconstituted specimens. This is in contrast to the simplified stress-based procedures wherein in-situ test metrics are the primary parameters used to evaluate liquefaction potential, with laboratory index tests and grain size distribution analyses having supporting roles if their performance is deemed necessary (e.g., use of measured fines content, FC, versus apparent FC in conjunction with the Cone Penetration Test, CPT, stress-based simplified procedure).

Herein an alternative approach to implementing the Dobry et al. [11] strain-based procedure is proposed which circumvents the need for

* Corresponding author.
E-mail addresses: eduardo3@vt.edu (E. Rodriguez-Arriaga), rugreen@vt.edu (R.A. Green).

https://doi.org/10.1016/j.soildyn.2018.05.033
Received 15 August 2017; Received in revised form 26 April 2018; Accepted 30 May 2018

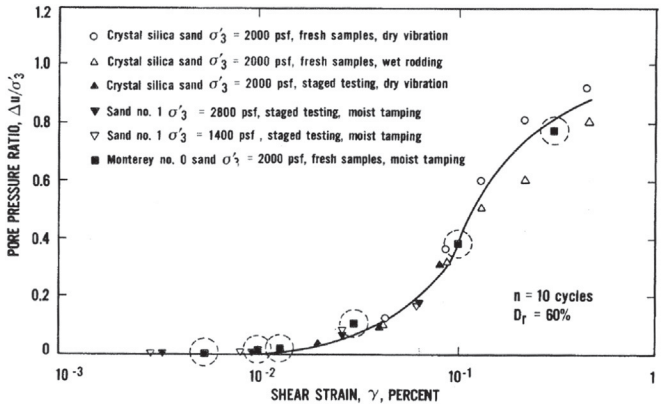

Fig. 1. Porewater pressure buildup in cyclic triaxial strain-controlled tests, after ten loading cycles, as a function of cyclic shear strain, for various normally consolidated saturated sands at D_r = 60% and for various pressures (Dobry et al. [11]).

performing strain-controlled cyclic laboratory tests. Per this procedure, a strain-based numerical excess pore pressure generation model is used in lieu of developing analogous relationships from laboratory tests. The soil parameters required to implement the procedure include: relative density (D_r), secant shear modulus (G), and grain size distribution characteristics of the soil (i.e., FC and coefficient of uniformity: C_u); note that focus herein is on soils that are susceptible to liquefaction (i.e., non-plastic soils) and thus Plasticity Index (PI) is not needed. These required parameters are not too different from those required to implement the stress-based simplified procedures and can be estimated using simple relationships or conservative assumptions.

To assess the efficacy of the proposed variant of the Dobry et al. [11] strain-based procedure, earthquake liquefaction case histories in the small strain shear wave velocity (V_s) database, which consists of 415 case histories compiled by Kayen et al. [20], and in the Standard Penetration Test (SPT) database, which consists of 230 case histories compiled by Boulanger et al. [2], are evaluated. Accordingly, the efficacy of the strain-based procedure can be assessed both in an absolute sense (i.e., with respect to field observations) and in a relative sense (i.e., relative to the efficacy of stress-based procedures). Additionally, using the two types of liquefaction case history databases in the assessment allows the significance of using one type of in-situ test metric, versus the other, to estimate needed parameters.

The following sections present the background information related to both the cyclic stress and cyclic strain approaches. Next, the steps used to implement the proposed variant of the strain-based procedure are outlined, and an overview of the liquefaction case history databases used in the assessment is given. The results from the assessment are then presented and discussed.

2. Background information

2.1. Liquefaction evaluation procedures

2.1.1. Simplified stress-based approach

As stated in the Introduction, the simplified stress-based procedure is widely used for evaluating liquefaction triggering. Per this procedure the seismic demand is quantified in terms of Cyclic Stress Ratio (CSR), which is the cyclic shear stress (τ_c) imposed at a given depth in the soil profile normalized by the initial vertical effective stress (σ'_{vo}) at that same depth. The word "simplified" in the procedure's title originated from the proposed use of a form of Newton's Second Law to compute τ_c at a given depth in the profile, in lieu of performing numerical site response analyses. The resulting "simplified" expression for CSR is:

$$CSR = \frac{\tau_c}{\sigma'_{vo}} = 0.65\left(\frac{a_{max}}{g}\right)\left(\frac{\sigma_v}{\sigma'_{vo}}\right)r_d \quad (1)$$

where: a_{max} = maximum horizontal acceleration at the ground surface; g = acceleration due to gravity; σ_v and σ'_{vo} = total and initial effective vertical stresses, respectively; and r_d = depth-stress reduction factor that accounts for the non-rigid response of the soil profile.

Additional factors are applied to Eq. (1), the need for which were largely based on results from laboratory studies, to account for durational effects of the shaking (MSF: Magnitude Scaling Factor, where the reference motion duration is for a moment magnitude 7.5 earthquake, M_w7.5), initial effective overburden stress (K_σ, where the reference initial effective overburden stress is 1 atm), and initial static shear stress (K_α, where the initial static shear stress is zero, e.g., level ground conditions). The resulting expression for the normalized CSR (i.e., CSR*: CSR normalized for motion duration for a M_w7.5 event, 1 atm initial effective overburden stress, and level ground conditions) is given by Eq. (2):

$$CSR^* = \frac{CSR}{MSF \bullet K_\sigma \bullet K_\alpha} = 0.65\left(\frac{a_{max}}{g}\right)\left(\frac{\sigma_v}{\sigma'_{vo}}\right)r_d\frac{1}{MSF \bullet K_\sigma \bullet K_\alpha} \quad (2)$$

Case histories compiled from post-earthquake investigations were categorized as either "Liquefaction" or "No Liquefaction," based on whether evidence of liquefaction was or was not observed at the sites. By plotting CSR* for each of the case histories as a function of the corresponding in-situ test metric (e.g., SPT N-value or V_s), normalized for clean sand conditions and an initial effective overburden stress of 1 atm etc., it can be observed that the "Liquefaction" and "No Liquefaction" cases tend to lie in two different regions of the graph. The "boundary" separating these two sets of case histories is referred to as the Cyclic Resistance Ratio ($CRR_{M7.5}$) and represents the capacity of the soil to resist liquefaction during an M_w7.5 event. This boundary can be expressed as a function of the normalized in-situ test metrics.

Consistent with the conventional definition for factor of safety (FS), the FS against liquefaction (FS_{Liq}) is defined as the capacity of the soil to resist liquefaction divided by the seismic demand:

$$FS_{Liq} = \frac{CRR_{M7.5}}{CSR^*} \quad (3)$$

As discussed subsequently in this paper, the efficacies of the deterministic variants of the Kayen et al. [20] V_s-based and Idriss and Boulanger [17] SPT-based simplified liquefaction evaluation procedures are used herein to compare with that of the proposed variant of the Dobry et al. [11] strain-based procedure.

2.1.2. Dobry et al. [11] strain-based approach

Early studies showed that volumetric strain in a given soil subjected to cyclic loading under drained conditions almost uniquely correlates with the amplitude of the applied cyclic shear strain (γ_c), rather than the applied τ_c (e.g., Silver and Seed [36]). The corollary of this finding is that the excess pore pressure ratio (r_u: $r_u = \Delta u/\sigma'_{vo}$, where Δu is the excess pore water pressure) in a given saturated soil subjected to cyclic loading under undrained conditions almost uniquely correlates with the amplitude of the applied γ_c, rather than the applied τ_c (e.g., Martin et al. [25]). Building on these findings, Dobry et al. [11] proposed a strain-based approach for evaluating liquefaction triggering potential, as an alternative to the stress-based approach.

Starting with the simplified equation to compute τ_c, Dobry et al. [11] proposed a simplified equation to compute γ_c:

$$\gamma_c = \frac{\tau_c}{G} \quad (4)$$

$$\gamma_c = 0.65\left(\frac{a_{max}}{g}\right)\frac{\sigma_v r_d}{G_{max}(G/G_{max})_{\gamma_c}} \quad (5)$$

where: G = secant shear modulus of the soil; G_{max} = small-strain ($\gamma_c \leq 10^{-4}$%) secant shear modulus of the soil; and $(G/G_{max})_{\gamma c}$ = normalized

secant shear modulus reduction ratio of the soil corresponding to γ_c. Dobry et al. [11] found that there is a limiting value of γ_c, below which no excess pore water pressures develop, regardless of the number of applied load cycles (n_{eq}); they referred to this limiting value of γ_c as the threshold volumetric shear strain (γ_{tv}). Dobry et al. [11] found that for normally consolidated clean and silty sands $\gamma_{tv} \approx 0.01\%$.

The strain-based liquefaction triggering evaluation procedure proposed by Dobry et al. [11] consists of four steps:

Step 1.. *Determination of γ_c and n_{eq}. γ_c is calculated using Eq. 5; the equivalent number of cycles, n_{eq}, can be obtained from established correlations with earthquake parameters.*

Step 2.. *Comparison between γ_c and the threshold strain of the soil, γ_{tv}. If $\gamma_c < \gamma_{tv}$, neither pore pressure buildup nor liquefaction will occur and the evaluation ends here.*

Step 3.. *If $\gamma_c > \gamma_{tv}$, the values of γ_c and n_{eq} are used in conjunction with experimental curves developed from strain-controlled cyclic tests performed on undisturbed and/or reconstituted samples prepared to the same relative density (D_r) as the soil in-situ (e.g., Fig. 1) to estimate r_u at the end of earthquake shaking.*

Step 4.. *The value of r_u estimated in Step 3 is used to decide if the site will experience initial liquefaction ($r_u \approx 1.0$) or not ($r_u < 1.0$).*

Laboratory studies performed around the same time Dobry et al. [11] published their procedure showed that the cyclic resistance of reconstituted soil samples prepared to a given D_r was heavily dependent on the sample preparation method (e.g., Mitchell et al. [30]). However, these studies based their findings on stress-controlled cyclic test data, while the experimental curves required to be developed in Step 3 should be based on strain-controlled cyclic test data. Unlike stress-controlled tests, the cyclic resistance of a given soil prepared to a given D_r determined using strain-controlled tests is relatively insensitive to method used to reconstitute the sample. The reason for this is that the sample preparation method inherently influences the sample stiffness. Accordingly, for a given applied shear stress, the amplitudes of the shear strains induced in samples prepared by different methods will differ, and excess pore pressure generation (and liquefaction) is a strain phenomenon.

3. Proposed alternative implementation of the Dobry et al. [11] strain-based procedure

3.1. Determination of γ_c and n_{eq}

Step 1 of the Dobry et al. [11] strain-based procedure is to determine γ_c and n_{eq}, which represents the amplitude and duration of the applied earthquake loading. In Eq. (5), the stiffness of the soil is represented by G_{max}·$(G/G_{max})_{\gamma c}$, where G_{max} can be computed from V_s and relationships for G/G_{max} as a function of γ_c have been proposed by several investigators (Fig. 2). These relationships often include predictive variables such as mean effective confining stress (σ'_{mo}), PI, overconsolidation ratio (OCR), etc. (e.g., Ishibashi and Zhang [18]; Darendeli [10]; and Menq [29]). However, because the G/G_{max} relationships are expressed as a function of γ_c, an iterative procedure is required to determine $(G/G_{max})_{\gamma c}$ and hence γ_c using Eq. (5).

Herein the G/G_{max} relationship proposed by Ishibashi and Zhang [18] is used to compute γ_c. Although more recent relationships have been proposed by Darendeli [10] and Menq [29], these relationships require predictive variables that are not provided in the liquefaction case history databases. Moreover, a parametric study was performed by the authors wherein reasonable values were assumed for the required predictive variables for the Darendeli [10] relationship for several case histories. The differences in the resulting computed excess pore water pressure ratios using the Ishibashi and Zhang [18] relationship versus Darendeli [10] relationship were not significant.

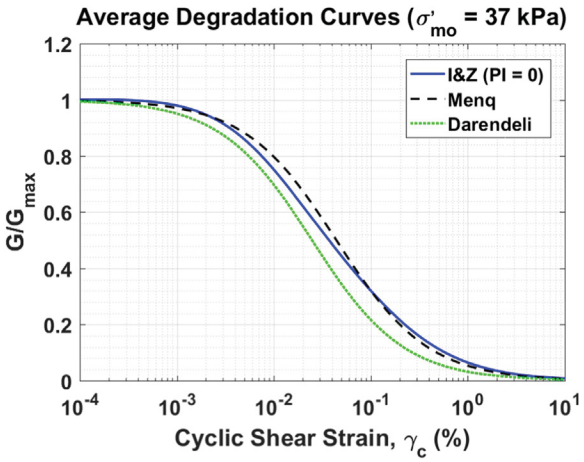

Fig. 2. Comparison of normalized shear modulus degradation curves using the Ishibashi and Zhang [18], Darendeli [10], and Menq [29] for clean sand.

In using Eq. (5) to compute γ_c in this study, the r_d relationship proposed by Lasley et al. [21] for active, shallow crustal tectonic regimes (e.g., western United States: WUS) was employed. This relationship is given by the following expressions:

$$r_d = (1-\alpha)\exp\left(\frac{-z}{\beta}\right) + \alpha \tag{6a}$$

$$\alpha = \exp(-4.373 + 0.4491 \cdot M_w) \tag{6b}$$

$$\beta = -20.11 + 6.247 \cdot M_w \tag{6c}$$

where: α = limiting value of r_d at large depths and can range from 0 to 1; β controls the curvature of the functions at shallow depths; and z = depth in meters.

3.1.1. Ishibashi and Zhang [18] normalized shear modulus reduction curve

The Ishibashi and Zhang [18] modulus reduction curve relationship is given by:

$$\frac{G}{G_{max}} = K(\gamma_c, PI)\sigma'^{\,m(\gamma_c, PI)-m_o}_{mo} \tag{7a}$$

$$m(\gamma_c, PI) - m_o = 0.272\left[1-\tanh\left\{\ln\left(\frac{0.000556}{\gamma_c}\right)^{0.4}\right\}\right]e^{-0.0145PI^{1.3}} \tag{7b}$$

$$K(\gamma_c, PI) = 0.5\left[1+\tanh\left\{\ln\left(\frac{0.000102+n(PI)}{\gamma_c}\right)^{0.492}\right\}\right] \tag{7c}$$

$$n(PI) = \begin{cases} 0.0 & PI = 0 \\ 3.37 \cdot 10^{-6} PI^{1.404} & 0 < PI \leq 15 \\ 7.0 \cdot 10^{-7} PI^{1.976} & 15 < PI \leq 70 \\ 2.7 \cdot 10^{-5} PI^{1.115} & PI > 70 \end{cases} \tag{7d}$$

where $K(\gamma_c, PI)$ is a decreasing function of γ_c, and $m(\gamma_c, PI)$ is an increasing function of γ_c. Both $K(\gamma_c, PI)$ and $m(\gamma_c, PI)$ were obtained from statistical regression of experimental data. The initial mean effective confining stress is computed as:

$$\sigma'_{mo} = \frac{\sigma'_{vo}(1 + 2K_o)}{3} \tag{8}$$

where K_o is the at-rest lateral earth pressure coefficient, which for normally consolidated, loose sands can be assumed to be 0.5 or can be estimated using relationships such as that proposed by Jaky [19].

In using Eq. (7) to compute $(G/G_{max})_{\gamma c}$ and γ_c in this study, PI = 0 was assumed because the soils analyzed are non-plastic. Also, a convergence criterion of 0.05% between γ_c values computed in sequential iterations was used.

3.1.2. Number of equivalent cycles, n_{eq}

Per Step 1 of the Dobry et al. [11] strain-based procedure, n_{eq} of the earthquake loading is required, which Dobry et al. [11] states is a function of earthquake magnitude. At the time of the writing of Dobry et al. [11], a few relationships for equivalent number of stress cycles ($n_{eq\tau}$) had been developed (e.g., Seed et al. [38]), but the authors are not aware of any equivalent number of strain cycles ($n_{eq\gamma}$) relationships having had been developed. Accordingly, Dobry et al. [11] likely assumed that $n_{eq\tau}$ and $n_{eq\gamma}$ were equivalent, which is not necessarily the case (e.g., Green and Terri [13]). Even today, few relationships have been developed for $n_{eq\gamma}$ (e.g., Green and Lee [14]; Chen et al. [7]; Lee and Green [24]), and these relationships were developed for evaluating seismic compression in dry or partially saturated soils, not for evaluating liquefaction in saturated soils.

Despite its questionable applicability for use in a strain-based liquefaction evaluation procedure, the $n_{eq\tau}$ relationship proposed by Lasley et al. [22] is used herein. The reason for selecting this relationship is because it was more rigorously developed than other existing $n_{eq\tau}$ and $n_{eq\gamma}$ relationships and none of the alternative relationships are any more applicable for use in the strain-based liquefaction procedure than the Lasley et al. [22] relationship.

Lasley et al. [22] built upon the work by Green and Terri [13] and Lee [23] and developed their relationship for earthquake magnitudes between 4.9 and 7.9 in shallow crustal active tectonic regions. To account for multidirectional shaking, Green and Terri [13] performed one-dimensional, equivalent linear site response analyses for each horizontal component in a pair of motions, added the energy dissipated at the respective depths for each component of motion, and set the amplitude of the equivalent cycle to 0.65 times the geometric mean of the maximum shear stresses experienced at a given depth. The same process of accounting for multidirectional shaking was used by Lasley et al. [22] and is referred to as Approach 2. With this Approach, $n_{eq\tau}$ represents the combined influence of both horizontal components of motion, with the resulting relationship given as:

$$\ln(n_{eq\tau}) = 0.4605 - 0.4082 \cdot \ln(a_{max}) + 0.2332 \cdot M_w \quad (9)$$

where a_{max} is the same as defined previously and has units of g. This correlation shows a negative correlation between $n_{eq\tau}$ and a_{max}, as shown in Fig. 3.

3.2. Threshold shear strain (γ_{tv}) and threshold peak ground acceleration, $(a_{max})_t$

Step 2 of the Dobry et al. [11] strain-based procedure determines whether $\gamma_c < \gamma_{tv}$. As stated previously, for normally consolidated clean and silty sands $\gamma_{tv} \approx 0.01\%$ (e.g., Silver and Seed [36]; Youd [45]; Stoll and Kald [39]; Dobry et al. [11]; Vucetic [42]; Abdoun et al. [1]; among others). This strain value was determined experimentally where the results of cyclic testing showed that when $\gamma_c \leq 0.01\%$ no excess pore water pressures were generated, even when subjected to a large number of cycles. In addition, Dobry et al. [11] presented analytical results, using a simple cubic array of quartz spheres, where the calculations also showed $\gamma_{tv} \approx 0.01\%$. Consistent with published studies, γ_{tv} was taken to be 0.01% in this assessment.

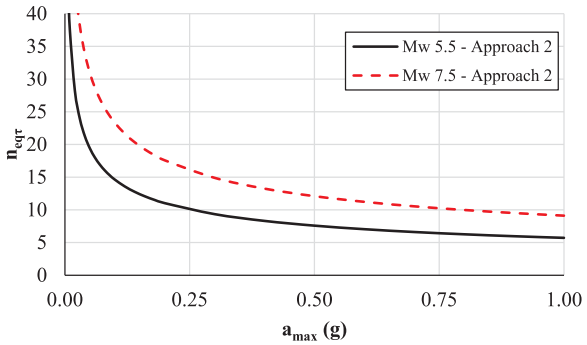

Fig. 3. Values of $n_{eq\tau}$ predicted with the Lasley et al. [22] correlation.

To provide a simple and fast screening method to determine whether or not the cyclic shear strain exceeds the threshold strain, Eq. (5) was used to develop a relationship for the peak ground surface acceleration required to induce a γ_c at a given depth in the soil profile equal to γ_{tv}. This acceleration is referred to as the threshold peak ground surface acceleration, $(a_{max})_t$, and below this value no excess pore pressures develop; $(a_{max})_t$ is expressed as:

$$(a_{max})_t = 0.000154 \frac{G_{max}(G/G_{max})_{\gamma_{tv}}}{\sigma_v r_d} \quad (10)$$

where $(a_{max})_t$ is in units of g; and $(G/G_{max})_{\gamma tv}$ = normalized shear modulus reduction ratio of the soil corresponding to γ_{tv}.

3.3. Excess pore pressure generation for $\gamma_c > \gamma_{tv}$

Step 3 of the Dobry et al. [11] strain-based procedure considers the scenario when $\gamma_c > \gamma_{tv}$. For this scenario, excess pore pressures will develop in the soil, and the magnitude of the generated excess pore pressures need to be estimated to determine whether liquefaction will be triggered. In lieu of developing a relationship between r_u and γ_c from laboratory tests, herein it is proposed that a strain-based numerical pore pressure generation model be used for this purpose. Specifically, the model proposed by Vucetic and Dobry [41] is used herein.

Vucetic and Dobry [41] developed an empirical relationship among r_u, γ_c, and $n_{eq\gamma}$ from undrained, strain-controlled cyclic shear test data on clean sands. Their model is given as:

$$r_u = \frac{p \cdot f \cdot n_{eq\gamma} \cdot F \cdot (\gamma_c - \gamma_{tv})^s}{1 + f \cdot n_{eq\gamma} \cdot F \cdot (\gamma_c - \gamma_{tv})^s} \quad (11)$$

where: r_u = residual excess pore pressure ratio after $n_{eq\gamma}$ cycles of applied loading; f = 1 or 2 for one- or two-dimensional loading, respectively; and p, F, and s are curve-fitting constants. The variable f was taken to be unity in this study because the Lasley et al. [22] correlation for $n_{eq\tau}$ combines the influence of both horizontal components of motion.

Mei et al. [28] proposed empirical correlations for the three curve-fitting parameters (p, F, and s) to avoid the need of performing laboratory cyclic testing to calibrate the model. Mei et al. [28] suggested setting p = 1 and s = 1 based on the analysis of data from laboratory cyclic tests that they performed and from others (Dobry et al. [12]; Vucetic and Dobry [41]; and Matasovic [26]). Additionally, Mei et al. [28] developed a correlation relating F, D_r, and C_u. They noted that F reflects the rate of Δu generation and should be inversely related to D_r and directly related to C_u. Fig. 4 shows their proposed correlation for clean, subangular to subrounded silica sands. Alternatively, F can be estimated using the correlation proposed by Carlton [4], which related F to V_s. This correlation is shown in Fig. 5. Finally, Mei et al. [28] refer to Dobry et al. [11], stating that γ_{tv} is usually between 0.01% and 0.02% for most sands; herein, $\gamma_{tv} = 0.01\%$ is assumed in implementing the Vucetic and Dobry [41] model.

A comparison of predicted and measured excess pore pressures is shown in Fig. 6. In this figure, the excess pore pressures were predicted using the model proposed by Vucetic and Dobry [41] model (C_u = 2.1 and D_r = 60%) and the measured pore pressures are from Dobry et al. [11] for strain-controlled cyclic triaxial tests performed on samples having D_r = 60%. As may be observed from this figure the Vucetic and Dobry [41] model gives a reasonable prediction of the measure pore pressures. Furthermore, Fig. 7 shows predicted excess pore pressures using the Vucetic and Dobry [41] model for loose (D_r = 30%) and medium dense (D_r = 60%) soils having σ'vo = 100 kPa for increasing values of n_{eqg}. As expected, ru increases more rapidly in looser soils than denser soils when subjected to the same loading. Also, for a given

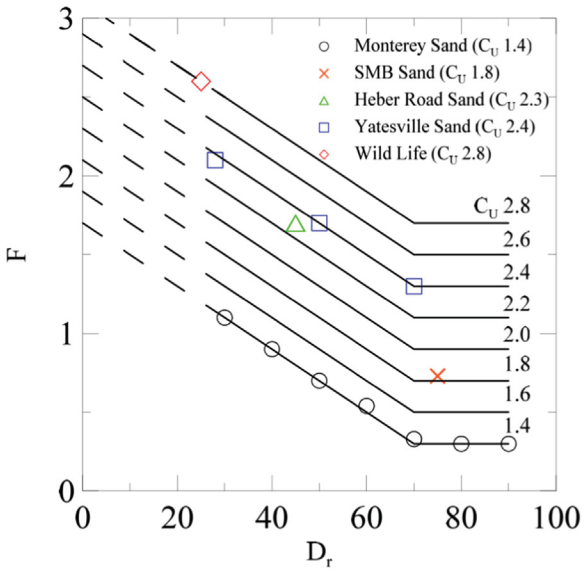

Fig. 4. Proposed correlation to estimate curve-fitting parameter F for the Vucetic and Dobry [41] model (Mei et al. [28]).

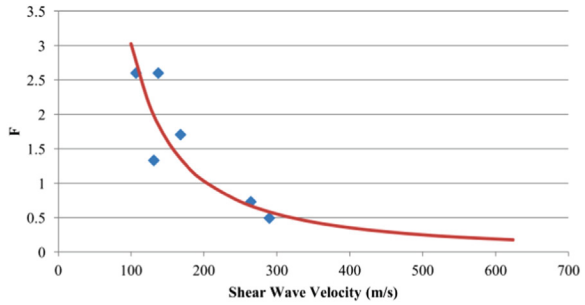

Fig. 5. Correlation between F and V_s (Matasovic and Ordóñez [27]; Carlton [4]).

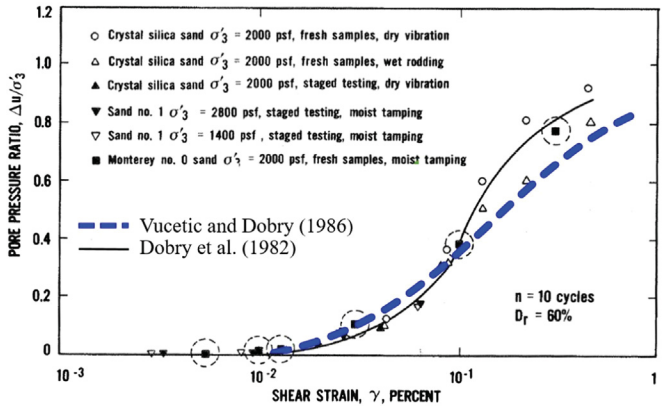

Fig. 6. A comparison of predicted and measured excess pore pressures, where Vucetic and Dobry [41] model (C_u = 2.1 and D_r = 60%) was used to predict the pore pressures and the measured pore pressures are from Dobry et al. [11] for strain-controlled cyclic triaxial tests performed on samples having D_r = 60%.

sample subject to a given amplitude g_c, r_u increases as n_{eqg} increases.

3.4. Assessing whether liquefaction is triggered

The final step in the Dobry et al. [11] strain-based procedure (i.e., Step 4) is to evaluate whether liquefaction is triggered. Dobry et al. [11] defined liquefaction as r_u = 1; therefore, a value of r_u computed from Step 3 that is less than 1 implies that liquefaction is not triggered. However, depending on the density of the soil, r_u < 1 can still result in damage to nearby infrastructure. Accordingly, as discussed subsequently, defining liquefaction by an $r_u \leq 1.0$ is considered appropriate. Note that r_u is unknown for the vast majority, if not all, the field case histories used to develop the stress-based liquefaction procedures; for these case histories, surficial manifestations, not r_u, were used to infer whether liquefaction was triggered or not.

3.5. Analyzing field case histories

The efficacy of the alternative implementation of the Dobry et al. [11] strain-based procedure is assessed by analyzing field case histories compiled by Kayen et al. [20] and Boulanger et al. [2]. Both the Kayen et al. [20] and the Boulanger et al. [2] databases include information about a_{max}, σ'_{vo}, σ_v, and depth of the critical layer for each case histories. The approaches used to estimate the other required parameters are outlined in the following sections on the respective case history databases. Also, additional information about the liquefaction case history databases used in this study is provided in the electronic supplement.

3.5.1. Kayen et al. [20], V_s database

The Kayen et al. [20] V_s liquefaction case history database is composed of 415 case histories, where V_s measurements were mainly made using the spectral analysis of surface waves method (SASW). Out of the 415 cases, 287 were catalogued as "Liquefaction" cases, 124 were catalogued as "No Liquefaction" cases, and four cases were considered to be on the margin between liquefaction and no liquefaction (i.e., "Marginal" cases). The case histories are from 34 earthquakes from sites in Japan (223 cases), the United States (105 in California, 24 in Idaho, and 9 in Alaska), China (30), Taiwan (20), Greece (2), and Turkey (2). Some of these sites are the same ones compiled in the SPT database by Cetin et al. [5] and the CPT database by Moss et al. [31].

To implement the alternative form of the Dobry et al. [11] strain-based procedure to evaluate the V_s case histories, the total unit weight (γ_t) of the critical layer needs to be estimated to compute G_{max} from the listed value of V_s:

$$G_{max} = \left(\frac{\gamma_t}{g}\right) V_s^2 \tag{12}$$

However, the Kayen et al. [20] database does not list values of γ_t for the critical layer. Assuming that most of the soils below the ground water table at the case history sites were sands or silty sands, the values of γ_t were approximated in the range from 16 to 20.5 kN/m^3 (100–130 lbs/ft^3) to match the reported values of σ'_{vo} and σ_v listed in the database.

3.5.2. Boulanger et al. [2], SPT database

The Boulanger et al. [2] SPT database is composed of 230 case histories, where 115 were catalogued as "Liquefaction" cases, 112 were catalogued as "No Liquefaction" cases, and three cases were considered "Marginal." The case histories are from 22 earthquakes from sites in Japan (150 cases), the United States (59 in California), China (11), Argentina (5), Guatemala (3), and Philippines (2).

To implement the alternative form of the Dobry et al. [11] strain-based procedure to evaluate the SPT case histories, the following parameters need to be estimated:

- G_{max} to compute γ_c.
- D_r and C_u to determine the F parameter for the Vucetic and Dobry [41] excess pore pressure generation model using the correlation proposed by Mei et al. [28].

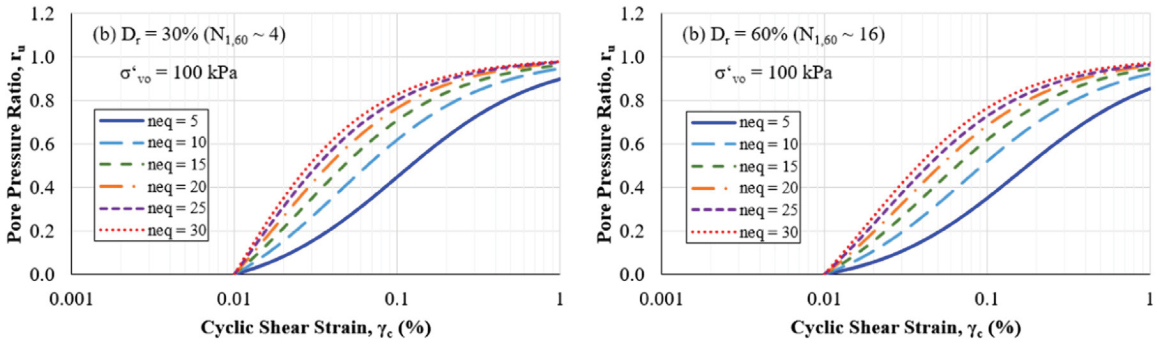

Fig. 7. Curves of pore pressure ratio versus cyclic shear strain at different numbers of equivalent cycles for loose and medium dense soils using the Vucetic and Dobry [41] model.

To estimate V_s for each of the SPT case histories, the relationship proposed by Wair et al. [42] for all Holocene aged soils is used:

$$V_s = 26.0 \bullet N_{60}^{0.215} \bullet \sigma'^{0.275}_{vo} \quad (13)$$

where V_s is in m/sec and σ'_{vo} is in kPa. Eq. (12) was then used to compute G_{max}, where γ_t was estimated using the same approach outlined above for the V_s case histories. The following relationship presented by Idriss and Boulanger [17] for sands was used to obtain D_r from corrected SPT N-value (i.e., $N_{1,60}$):

$$D_r = \sqrt{\frac{N_{1,60}}{46}} \quad (14)$$

where D_r is constrained between 30% and 90%. For all cases, an average value of C_u = 2.1 was assumed.

To account for fines in the soil, the "clean sands" correction was applied to $N_{1,60}$ (i.e., $N_{1,60cs}$) and used to estimate the needed parameters. However, due to the uncertainty in the appropriateness of this approach, a subset of the SPT case histories that have a FC ≤ 5% was analyzed separately from the entire SPT database. This subset consisted of 116 cases: 62 Liquefaction cases and 54 No Liquefaction cases.

4. Results

As detailed below, Steps 1–4 were followed for the alternative implementation of the strain-based procedure.

4.1. Determination of γ_c and $n_{eq\gamma}$

To compute γ_c for each case history, it was necessary to use an iterative approach in conjunction with the shear modulus degradation curves. Example results are shown for two case histories in Fig. 8. In implementing the iteration algorithm to compute γ_c, a maximum cap of 3% was imposed. This was done because it is doubtful that strains larger than this were induced in-situ solely as a result of earthquake shaking and the validity of the shear modulus degradation curves become questionable at larger strains. Rodriguez-Arriaga [35] provides the shear modulus degradation curves for all the case histories in the Kayen et al. [20] and Boulanger et al. [2] databases showing their corresponding converged values of γ_c. Plots of the γ_c values for all the case histories as a function of V_s (for the case histories in Kayen et al. [20]) and $N_{1,60cs}$ (for the case histories in Boulanger et al. [2]) are shown in the next section.

Eq. (9), proposed by Lasley et al. [22], was used to compute $n_{eq\tau}$ for each case history, consistent with the inherent assumption made by Dobry et al. [11] wherein $n_{eq\gamma}$ and $n_{eq\tau}$ are equivalent. The results are presented as a function of a_{max} and M_w in Figs. 9 and 10 for the Kayen et al. [20] and Boulanger et al. [2] databases, respectively.

4.2. Threshold shear strain (γ_{tv}) and threshold peak ground acceleration, $(a_{max})_t$

The computed γ_c values for both Kayen et al. [20] and Boulanger et al. [2] databases are shown in Fig. 11. As may be observed from this figure, the γ_c below which there are no "Liquefaction" cases are 0.03% and 0.05% for the Kayen et al. [20] and Boulanger et al. [2] databases, respectively. Note, however, these values of γ_c conceptually are not synonymous to γ_{tv} because it is unknown whether any pore pressures were generated in some of the "No Liquefaction" cases having γ_c less than these values.

As stated previously, to provide a simple and fast screening method

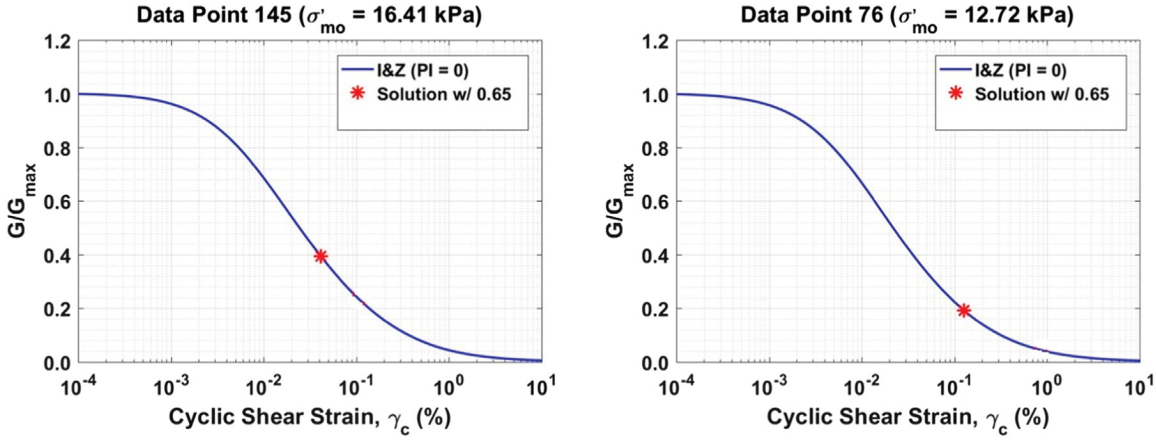

Fig. 8. Example of the converged solutions of cyclic shear strain using the Ishibashi and Zhang [18] shear modulus degradation curves with two case histories from the Kayen et al. [20] database.

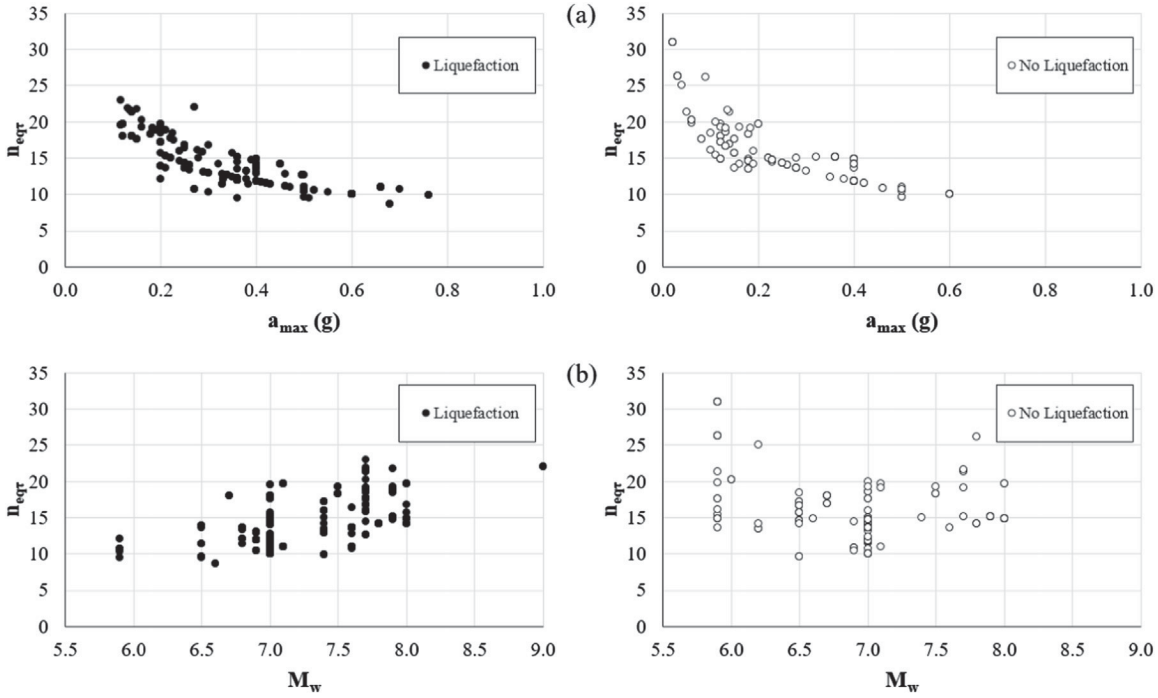

Fig. 9. Results of $n_{eq\tau}$ for the Kayen et al. [20] database as a function of (a) a_{max} and (b) M_w.

to determine whether or not the cyclic shear strain exceeds the threshold strain, the threshold peak ground surface acceleration can be compared with the a_{max} for the design earthquake motions. Fig. 12 shows a plot of the a_{max} values as a function of M_w for the case histories in the Kayen et al. [20] and Boulanger et al. [2] databases. As may be observed from this figure, the lowest a_{max} values for Liquefaction cases are approximately 0.12 and 0.09 g for the V_s and SPT databases, respectively. In comparison, the limiting values of $(a_{max})_t$ computed using Eq. (10), for the Kayen et al. [20] database is 0.12 g and for the Boulanger et al. [2] database is 0.08 g, which are very consistent with the limiting $(a_{max})_t$ values for both databases.

A summary of the computed γ_c, a_{max}, and $(a_{max})_t$ values for both the Kayen et al. [20] V_s database and the Boulanger et al. [2] SPT database are listed in Table 1.

4.3. Excess pore pressure generation for $\gamma_c > \gamma_{tv}$

For the cases where $\gamma_c > \gamma_{tv}$, the Vucetic and Dobry [41] pore pressure generation model is used in conjunction with the Lasley et al. [22] $n_{eq\tau}$ relationship to estimate r_u for the case histories compiled in

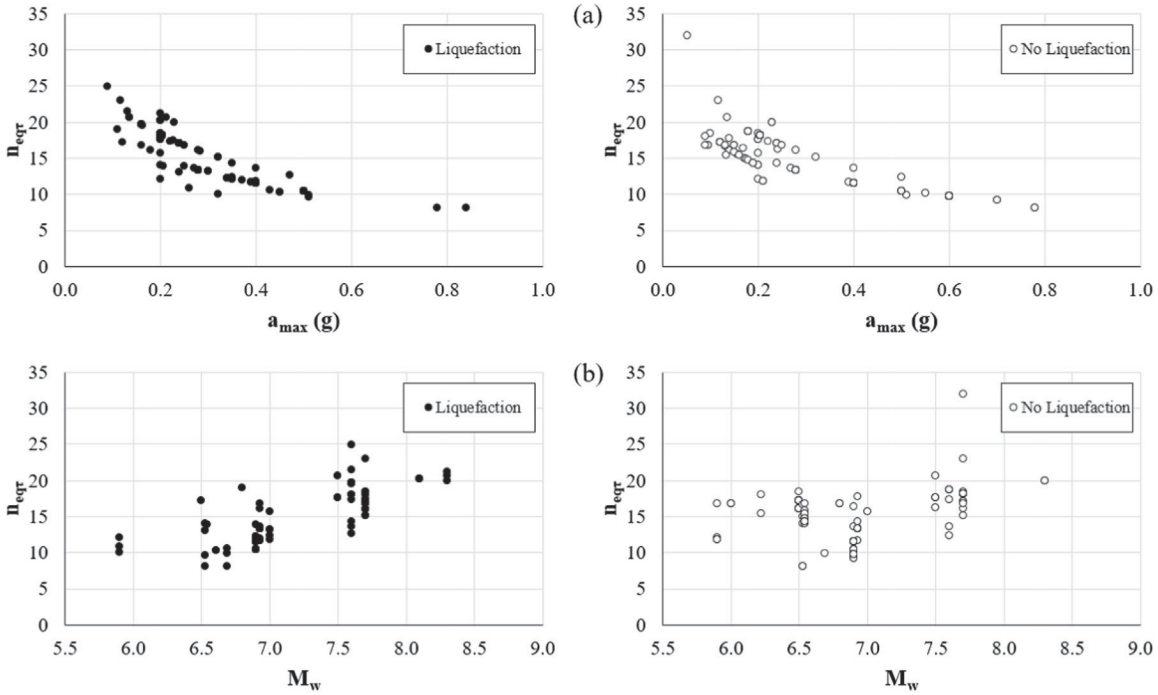

Fig. 10. Results of $n_{eq\tau}$ for Boulanger et al. [2] database as a function of (a) a_{max} and (b) M_w.

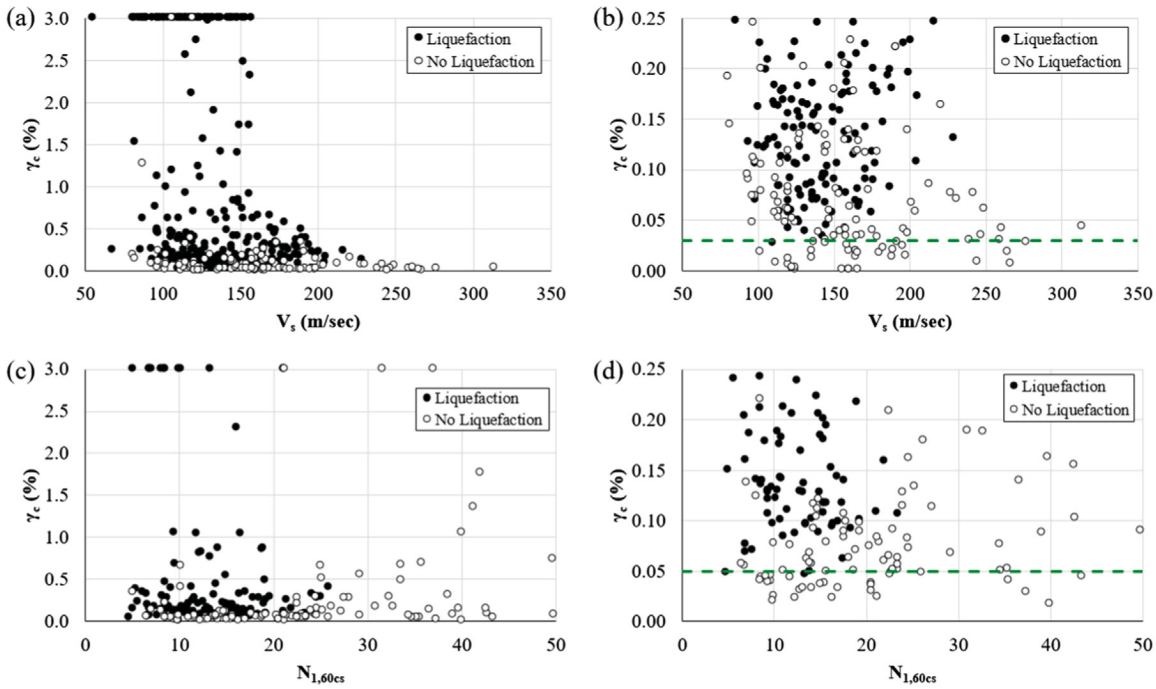

Fig. 11. (a) & (b) γc versus V_s for the Kayen et al. [20] database; and (c) & (d) γ_c versus $N_{1,60cs}$ for the Boulanger et al. [2] database; (b) and (d) are zoomed-in plots of (a) and (c).

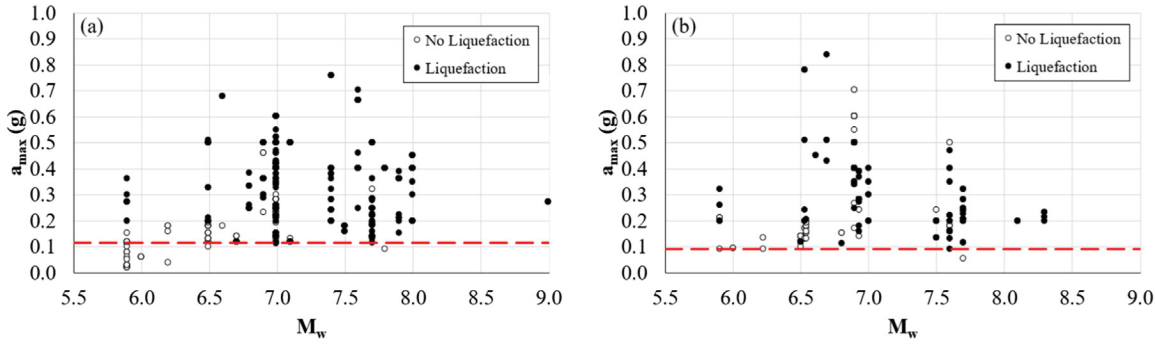

Fig. 12. Plots of a_{max} versus M_w for: (a) the Kayen et al. [20] V_s database; and (b) the Boulanger et al. [2] SPT database.

Table 1
Limiting values of γ_c, a_{max}, $(a_{max})_t$.

Database	Limiting Values		$(a_{max})_t$ (g)
	γ_c (%)	a_{max} (g)	
Kayen et al. [20]	0.03	0.12	0.12
Boulanger et al. [2]	0.05	0.09	0.08

the Kayen et al. [20] and Boulanger et al. [2] databases. In this study, the "Marginal" liquefaction case histories in the two databases (seven in total for the two databases) were treated as "Liquefaction" cases to simplify the reporting of results with a binary denomination of either "Liquefaction" or "No Liquefaction."

For the case histories in the Kayen et al. [20] V_s database, the Carlton [4] relationship is used to obtain F to calibrate the Vucetic and Dobry [41] model. Sample results for case histories having low (100 – 120 m/sec) and high (200 – 314 m/sec) V_s values are plotted in Fig. 13. A complete presentation of the r_u values computed for all the case histories in the Kayen et al. [20] database is given in Rodriguez-Arriaga [35].

As may be observed from Fig. 13, the case histories are grouped in bins based on $n_{eq\tau}$ (i.e., duration of cyclic loading). However, the cases are not separated based on σ'_{vo} because laboratory test results presented in Dobry et al. [11] showed that the vertical effective stress did not affect r_u generation for strain controlled loading. Also, the cases for $M_w > 7.9$ are identified with distinctly colored symbols since the Lasley et al. [22] $n_{eq\tau}$ correlation was not developed for these large magnitude events.

Analogous plots to those in Fig. 13 for the Kayen et al. [20] V_s database are shown in Fig. 14 for the Boulanger et al. [2] SPT database. A complete presentation of the r_u values computed for all the case histories in the Boulanger et al. [2] database is given in Rodriguez-Arriaga [35]. In analyzing the SPT case histories, the Wair et al. [43] correlation is used to estimate V_s values, which in turn are used to compute G_{max} values that are needed to compute γ_c per Eq. (5). Both D_r and C_u need to be estimated to determine the calibration coefficients for the Vucetic and Dobry [41] excess pore pressure generation model. Eq. (14) is used to estimate D_r and an average value of C_u is assumed (i.e., $C_u = 2.1$).

4.4. Assessing whether liquefaction is triggered

The final step in the alternative implementation of the Dobry et al.

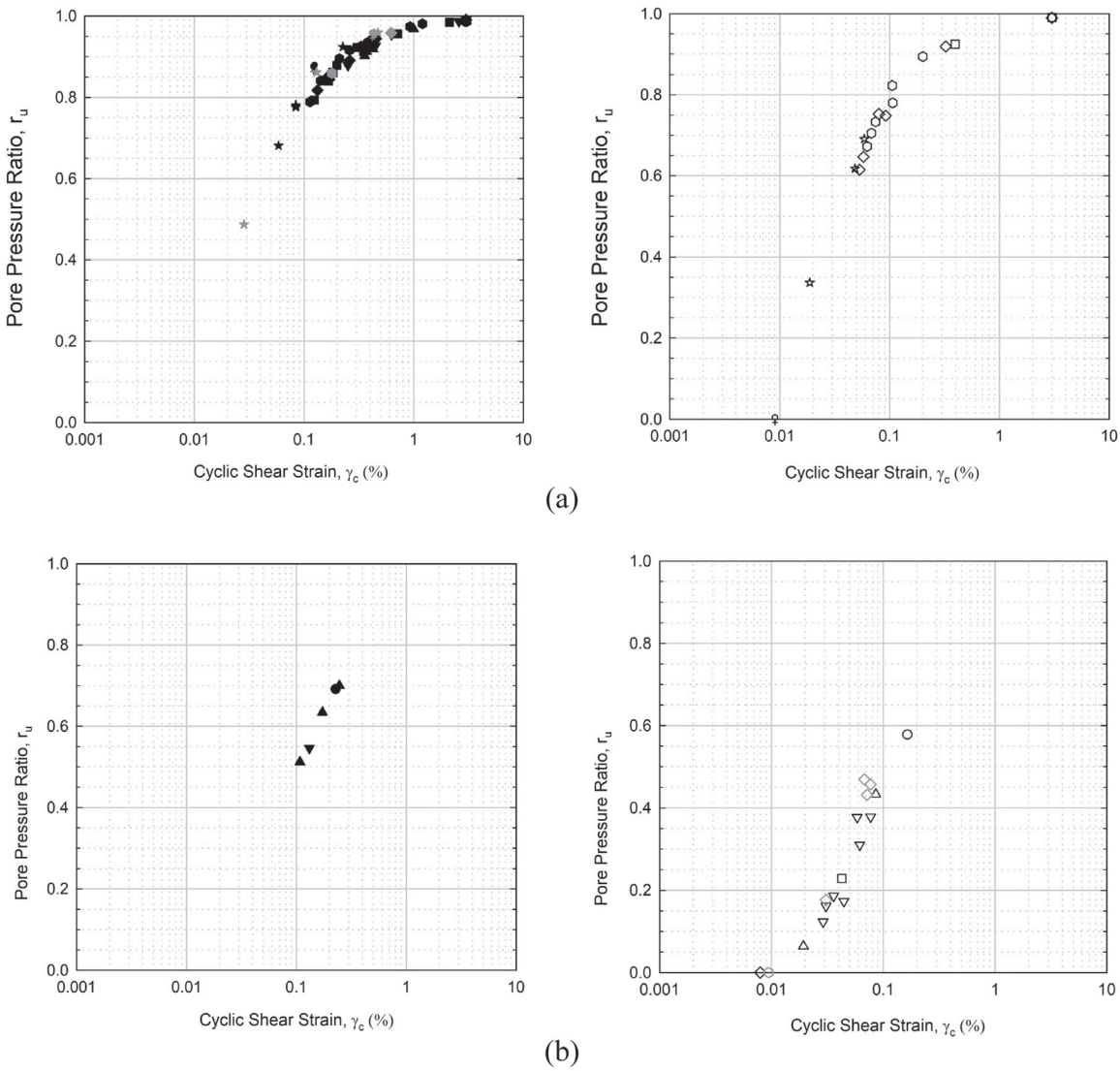

Fig. 13. Estimated r_u computed using the Vucetic and Dobry [41] model for sample case histories from the Kayen et al. [20] V_s database: (a) V_s = 100–120 m/sec; and (b) V_s = 200–314 m/sec.

[11] procedure is to assess the values of r_u computed in Step 3 to determine whether or not liquefaction is triggered. However, in interpreting the results from Step 3, the strict definition of liquefaction (i.e., r_u = 1) was relaxed some to a more pragmatic value of r_u = 0.95 which could potentially result in surficial manifestations. The results are listed in Table 2 in terms of True Positive, True Negative, False Positive, and False Negative, which are defined as:

- True Positive: liquefaction is predicted and was observed (i.e., it was a "Liquefaction" case).
- True Negative: liquefaction is not predicted and was not observed (i.e., it was a "No Liquefaction" case).
- False Positive: liquefaction is predicted but was not observed (i.e., it was a "No Liquefaction" case).
- False Negative: liquefaction is not predicted but was observed (i.e., it was a "Liquefaction" case).

Accordingly, True Positives and True Negatives are accurate predictions, False Positive is an inaccurate but conservative prediction, and False Negative is an inaccurate and unconservative prediction.

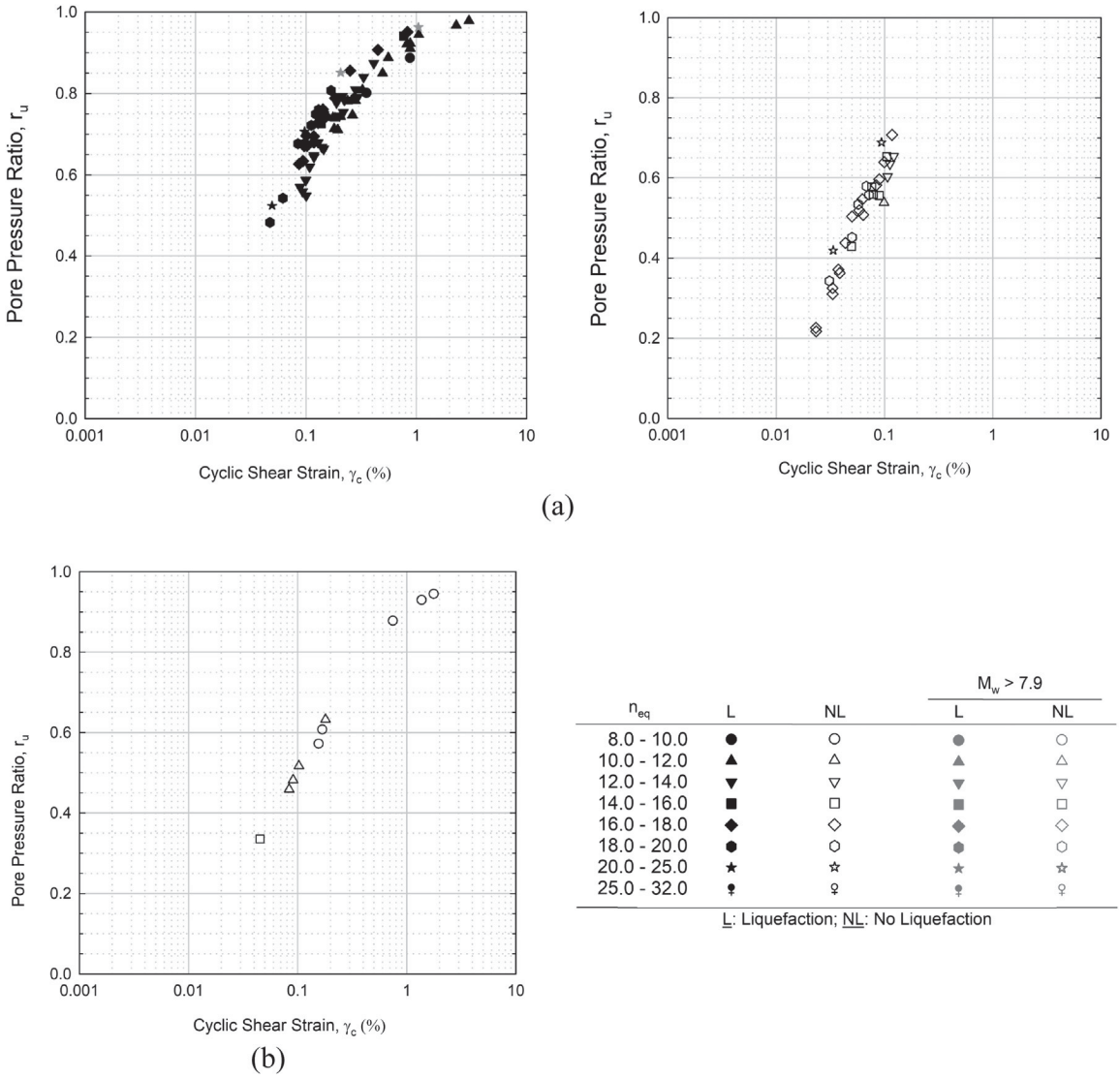

Fig. 14. Estimated r_u computed using the Vucetic and Dobry [41] model with the Boulanger et al. [2] SPT database: (a) $N_{1,60cs}$ = 10–20 blws/30 cm; and (b) $N_{1,60cs}$ = 40–50 blws/30 cm.

Table 2
Predictions versus field observations for both the strain- and stress-based procedures.

Database	**Kayen et al. [20] (415 cases)**		**Boulanger et al. [2] (230 cases)**		**Boulanger et al. [2] FC ≤ 5% (116 cases)**	
Approach	*Strain-based*	*Stress-based*	*Strain-based*	*Stress-based*	*Strain-based*	*Stress-based*
True Positive	24%	68%	6%	48%	6%	52%
True Negative	29%	19%	47%	39%	45%	38%
Accurate Predictions	**53%**	**87%**	**53%**	**87%**	**51%**	**90%**
False Positive	1%	11%	1%	10%	2%	8%
False Negative	46%	2%	46%	3%	47%	2%
Incorrect Predictions	**47%**	**13%**	**47%**	**13%**	**49%**	**10%**

5. Discussion

5.1. Cyclic shear strains and number of equivalent cycles

The "simplified" procedure to compute γ_c proposed by Dobry et al. [11] (i.e., Eq. (5)) assumes that $G_{max}{\cdot}(G/G_{max})_{\gamma c}$ is uninfluenced by the softening of the soil due to the generation of excess pore water pressures. However, this is known not to be the case when $\gamma_c > \gamma_{tv}$. Dobry et al. [11] allude to this, stating that "…some additional research is needed to develop definite rules for computing γ_c." The authors actually view this as an inherent and potentially fatal limitation of the strain-based procedure. The representation of chaotic earthquake ground motions in an "equivalently damaging" and simplified form requires the specification of the simplified motion's amplitude (e.g., γ_c) and duration (e.g., $n_{eq\gamma}$). If it is assumed that $G_{max}{\cdot}(G/G_{max})_{\gamma c}$ is uninfluenced by the generation of excess pore water pressures in computing γ_c, then the softening of the soil due to excess pore pressure generation needs to be accounted for in computing $n_{eq\gamma}$. However, assuming that $n_{eq\gamma}$ is equivalent to $n_{eq\tau}$, where the latter is computed using a "total stress" approach (e.g., Seed et al. [37]; Green and Terri [13]), does not satisfy this need. Furthermore, to the authors' knowledge, no existing $n_{eq\gamma}$ relationship accounts for the softening effects of the soil due to excess pore water, nor has any framework been proposed in literature on how to compute $n_{eq\gamma}$ that accounts for the softening effects of the soil due to excess pore water.

As an alternative to requiring $n_{eq\gamma}$ to account for the softening effects due to excess pore water pressure, γ_c could be computed for each

half cycle of loading using Eq. (5), wherein the effective confining stress used to compute G_{max}·$(G/G_{max})_{\gamma c}$, and hence γ_c, is updated to account for excess pore pressure generation each half cycle of loading. This would require that relationships such as that shown in Fig. 1 be generated for $n_{eq\gamma} = 0.5$ cycles. This is certainly feasible, but in essence, this is what the Byrne [3] strain-based pore pressure generation model does, with the Byrne [3] model being more versatile than the Dobry et al. [11] strain-based liquefaction evaluation procedure.

5.2. Threshold strains and accelerations

As listed in Table 1, the limiting values of γ_c (i.e., no "Liquefaction" case histories have γ_c values below the limiting values) differ for the V_s and SPT databases, and differ from γ_{tv}. However, the limiting value γ_c is simply the smallest induced shear strain for all of the "Liquefaction" case histories analyzed. This is not to say that no excess pore water pressures developed in the "No Liquefaction" case histories that had induced strains less than the limiting value of γ_c. A more correct interpretation of the data presented in Fig. 11 is that when $\gamma_c > 0.5\%$ liquefaction is very likely and when $\gamma_c < 0.03\%$ liquefaction is very unlikely, with this latter criterion being somewhat consistent with the $\gamma_{tv} \approx 0.01\%$ proposed by Dobry et al. [11]. Also, the disparity between the limiting values of γ_c and γ_{tv} could be due to the uncertainties in the various correlations used to estimate unknown parameters needed to compute γ_c. Furthermore, the ranges of the scenarios represented in the databases are limited (e.g., NRC [32]), and as a result, the lack of robustness of both databases is likely the most contributing factor for having differing values of γ_c for the two databases and γ_{tv}.

As a corollary to γ_{tv}, Dobry et al. [11] performed a parametric study to compute $(a_{max})_t$ for loose and dense soils, assuming the same value of total unit weight of the soil above and below the water table of 18 kN/m^3 (115 pcf) and $(G/G_{max})_{\gamma tv} = 0.75$. For the soil conditions that were "most susceptible to liquefaction," the lowest value of $(a_{max})_t$ they computed was 0.05 g, compared to 0.08 – 0.12 g determined herein from the analysis of the Boulanger et al. [2] and Kayen et al. [20] databases (Table 1). The difference between the results from the simple parametric study performed by Dobry et al. [11] and the results from the analyses of the field case histories presented herein do not differ significantly.

5.3. Liquefaction triggering predictions

Table 2 summarizes the statistics regarding the prediction accuracy of the alternative implementation of the Dobry et al. [11] strain-based procedure. In comparing the efficacies of the strain-based procedure implemented for cases where V_s is known and other parameters are estimated and for cases where $N_{1,60cs}$ is known and other parameters are estimated, the respective percentages of accurate (i.e., True Positives and Negatives) and inaccurate (i.e., False Positives and Negatives) predictions were identical for both the V_s versus $N_{1,60cs}$ case histories analyzed. However, there was a higher percentage of True Negative predictions when $N_{1,60cs}$ was known than when V_s was known; conversely there was a higher percentage of True Positive predictions when V_s was known than when $N_{1,60cs}$ was known. The authors are uncertain about why knowing $N_{1,60cs}$ results in more accurate predicts of the non-occurrence of liquefaction (i.e., True Negative) and knowing V_s results in more accurate prediction of the occurrence of liquefaction (i.e., True Positive). However, it could be related to the subjective positioning of the deterministic $CRR_{M7.5}$ curves for the respective procedures or the robustness of the scenarios represented in the respective case history databases. Regardless, issues related to using $N_{1,60cs}$ versus V_s to characterize the soil are:

- $N_{1,60cs}$ better correlates to D_r than does V_s; in contrast, V_s better correlates to void ratio (e.g., Richart et al. [34]) than $N_{1,60cs}$ does. As a result, two soils that have the same void ratio, but drastically different D_r, will likely have V_s values that are closer to each other than their $N_{1,60cs}$ values will be. Ultimately, D_r relates more to a soil's contractive tendencies when sheared and thus to a soil's liquefaction resistance than void ratio does. Hence, $N_{1,60cs}$ is likely a better in-situ test metric for correlating to liquefaction resistance than V_s is. Having said this, there are scenarios where characterizing soils in-situ using V_s may be preferred to using SPT (e.g., gravelly and cobbley soils).
- The Vucetic and Dobry [41] pore pressure generation model was developed for clean sands (i.e., sands with FC ≤ 5%). For the V_s case histories, FC were unknown and therefore ignored in implementing the strain-based procedure; this is clearly a shortcoming in implementing the procedure. However, for the SPT case histories, $N_{1,60cs}$ values (as opposed to $N_{1,60}$ values) were used to determine the calibration parameters for the pore pressure generation model. As mentioned previously, there is uncertainty about the appropriateness of doing this. To determine if this approach for accounting for FC impacted the accuracy of the strain-based procedure, a subset of the SPT case histories from Boulanger et al. [2] that have FC ≤ 5% was analyzed. This subset consisted of 116 cases (out of a total of 230 cases in the database): 62 "Liquefaction" cases and 54 "No Liquefaction" cases.

The prediction statistics for the clean sand SPT cases and the entire SPT database are presented in Table 2, and a complete presentation of the r_u computed for all the case histories in the Boulanger et al. [2] database, to include the subset having FC ≤ 5% is given in Rodriguez-Arriaga [35]. As may be observed from Table 2, the overall accuracy of the procedure decreases slightly from 53% to 51% when only clean sand case histories are analyzed, with the percentage of False Negative (i.e., inaccurate and unconservative predictions) remaining essentially the same. This implies that using $N_{1,60cs}$ to account for FC is reasonable.

Given that the strain-based procedure has been proposed as a potential alternative to the widely used stress-based procedures, the efficacy of the strain-based procedure needs to be compared with those of the stress-based procedures. Towards this end, Table 2 also includes the prediction statistics (i.e., percentages of True Positive, True Negative, False Positive, and False Negative) for both the Kayen et al. [20] and the Boulanger and Idriss [2] deterministic simplified stress-based procedures. From the values in Table 2, it can be observed that both of the stress-based procedures yield more accurate predictions (and hence fewer incorrect predictions) than the strain-based procedure, regardless of whether the SPT N-values or V_s is used as the in-situ test metric. However, it should be noted that the databases used to assess the efficacies of the stress-based procedures are essentially the same ones used to develop the $CRR_{M7.5}$ curves inherent to the respective procedures (i.e., the stress-based procedures were in essence "calibrated" using the databases), while this is not the case for the strain-based procedure. From this perspective the prediction statistics listed in Table 2 are inherently biased in favor of the stress-based procedures.

5.4. Additional uncertainties

The analyses performed in this study are inherently deterministic (i.e., liquefaction triggering is evaluated via alternative implementation of the strain-based procedure using best estimates of excess water pressure ratios and the deterministic versions of the SPT and V_s simplified stress-based procedures). As a result, to assess whether the epistemic uncertainty associated with certain aspects of the alternative implementation of the strain-based procedure has a significant influence on the trends noted above, parametric analyses were performed using the Byrne [3] strain-based pore pressure generation model (versus the Vucetic and Dobry [41] model), using the Darendeli [10] secant shear modulus degradation relationship (versus the Ishibashi and Zhang [18] relationship), and using a maximum cap of 1% on the computed γ_c (versus 3%) via the secant shear modulus degradation relationship. Of

these, the choice of the strain-based excess pore water pressure generation model has the biggest influence on the computed results, with the Byrne [3] model resulting in more accurate predictions than when the Vucetic and Dobry [41] model is used. However, even these improved predictions are still significantly less accurate than the predictions of the stress-based models. Finally, having measurements of both V_s and penetration resistance for sites being evaluated would undoubtedly improve the accuracy of the strain-based approach because there would be less reliance of correlations to estimate needed parameters. However, it is unknown whether this would significantly improve the efficacy of the procedure to make it competitive with the stress-based procedure.

6. Summary and conclusions

The existence of a volumetric threshold shear strain, below which there is no development of excess pore pressures, and the unique relationship between excess pore pressures and cyclic shear strain, make compelling arguments for adopting a strain-based approach for evaluating liquefaction potential. Herein an alternative implementation of the Dobry et al. [11] cyclic strain approach is assessed by evaluating liquefaction triggering using both V_s and SPT case histories. Toward this end, γ_c was computed using the Dobry et al. [11] procedure in conjunction with shear modulus degradation curves by Ishibashi and Zhang [18]. As a corollary to γ_{tv}, $(a_{max})_t$ was shown to provide a fast and simple screening for liquefaction triggering, where liquefaction triggering is unlikely when a_{max} is less than ~0.08–0.12 g, which corresponds to γ_c in the critical stratum less than ~0.03–0.05%.

If either $a_{max} > 0.08–0.12$ g or $\gamma_c > 0.03–0.05\%$, excess pore pressures are predicted to develop and it becomes necessary to quantify these pore pressures to evaluate liquefaction potential. This was accomplished by implementing the pore pressure generation model by Vucetic and Dobry [41], using correlations by Mei et al. [28] and Carlton [4] to obtain the required model calibration parameters and the correlation by Lasley et al. [22] to estimate $n_{eq\gamma}$. For the case histories analyzed, the efficacy of the strain-based procedure was identical when V_s versus $N_{1,60cs}$ are known and other parameters are estimated. However, there was a higher percentage of True Negative predictions when $N_{1,60cs}$ was known than when V_s was known; conversely there was a higher percentage of True Positive predictions when V_s was known than when $N_{1,60cs}$ was known. This could be related to the subjective positioning of the deterministic $CRR_{M7.5}$ curves for the respective procedures or the robustness of the scenarios represented in the respective case history databases.

In comparing the efficacies of the strain-based and stress-based procedures, it was observed that both of the stress-based procedures yielded more accurate predictions than the strain-based procedure, regardless of whether V_s or $N_{1,60cs}$ was used to characterized the soils in-situ. However, it should be noted that the databases used to assess the efficacies of the stress-based procedures are essentially the same ones used to develop the $CRR_{M7.5}$ curves inherent to the procedures, while this is not the case for the strain-based procedure. From this perspective the comparison of the efficacies was inherently biased in favor of the stress-based procedures. Additionally, the efficacy of the strain-based procedure significantly increased when the Byrne [3] strain-based excess pore pressure model was used in lieu of the Vucetic and Dobry [41] model, but was still significantly less than those of the stress-based procedures. One likely reason for the lack of accuracy in the strain-based procedure's predictions is the inherent and potentially fatal limitation of the procedure ignoring the softening of the soil stiffness due to excess pore pressure when representing the earthquake loading in terms of γ_c and $n_{eq\gamma}$.

Acknowledgements

This study is based on work supported in part by the U.S. National Science Foundation (NSF) grants CMMI-1030564, CMMI-1435494, and CMMI-1724575. The authors gratefully acknowledge this support. The authors also gratefully acknowledge the review comments by Professors Adrian Rodriguez-Marek and Dove and Ms. Kristin Ulmer of Virginia Tech, and to Professor Mladen Vucetic, UCLA for providing copies of reports that we were unable to obtain otherwise. However, any opinions, findings, and conclusions or recommendations expressed in this paper are those of the authors and do not necessarily reflect the views of NSF or of those who provided review comments or assisted in obtaining documents.

Appendix A. Supplementary material

Supplementary data associated with this article can be found in the online version at http://dx.doi.org/10.1016/j.soildyn.2018.05.033.

References

[1] Abdoun T, Gonzalez MA, Thevanayagam S, Dobry R, Elgamal A, Zeghal M, Mercado MV, El Shamy U. Centrifuge and large-scale modeling of seismic pore pressures in sands: cyclic strain interpretation. J Geotech Geoenviron Eng 2013;139(8):1215–34.
[2] Boulanger RW, Wilson DW, Idriss IM. Examination and reevaluation of SPT-based liquefaction triggering case histories. J Geotech Geoenviron Eng 2012;138(8):898–909.
[3] Byrne PM. A cyclic shear-volume coupling and pore pressure model for sand. Proceedings, 2nd International Conference on Recent Advances in Geotechnical Earthquake Engineering and Soil Dynamics, St. Louis, pp. 47-55.
[4] Carlton B. An improved description of the seismic response of sites with high plasticity soils, organic clays, and deep soft soil deposits. PhD Dissertation, Department of Civil and Environmental Engineering. Berkeley, CA: University of California; 2014.
[5] Cetin KO, Seed RB, Moss RES, Der Kiureghian A, Tokimatsu K, Harder Jr LF, Kayen RE. Field case histories for SPT-based in situ liquefaction potential evaluation. PEER Report No. UCB/GT-2000/09. Berkeley, CA: Pacific Earthquake Engineering Research; 2000.
[6] Cetin KO, Seed RB, Der Kiureghian A, Tokimatsu K, Harder Jr LF, Kayen RE, Moss RES. SPT-based probabilistic and deterministic assessment of seismic soil liquefaction potential. J Geotech Geoenviron Eng 2004;130(12):1314–40.
[7] Chen Q, Gao G, Green RA, Zhang L. Computation of equivalent number of uniform strain cycles for seismic compression of sand subjected to multidirectional Earthquake loading. World Earthq Eng 2010;26:6–12. [in Chinese].
[8] Cubrinovski M, Green RA. (eds.). Geotechnical Reconnaissance of the 2010 Darfield (Canterbury) Earthquake. (contributing authors in alphabetical order: J. Allen, S. Ashford, E. Bowman, B. Bradley, B. Cox, M. Cubrinovski, R. Green, T. Hutchinson, E. Kavazanjian, R. Orense, M. Pender, M. Quigley, and L. Wotherspoon). Bulletin of the New Zealand Society for Earthquake Engineering, 43(4): pp. 243–320; 2010.
[9] Cubrinovski M, Bradley B, Wotherspoon L, Green R, Bray J, Woods C, Pender M, Allen J, Bradshaw A, Rix G, Taylor M, Robinson K, Henderson D, Giorgini S, Ma K, Winkley A, Zupan J, O'Rourke T, DePascale G, Wells D. Geotechnical aspects of the 22 February 2011 Christchurch earthquake. Bull NZ Soc Earthq Eng 2011;43(4):205–26.
[10] Darendeli MB. Development of a new family of normalized modulus reduction and material damping curves. Ph.D. Dissertation, Department of Civil, Architectural, and Environmental Engineering, University of Texas, Austin, TX; 2001.
[11] Dobry R, Ladd R, Yokel F, Chung R, Powell D. Prediction of pore water pressure buildup and liquefaction of sands during earthquakes by the cyclic strain method. NBS Building Science Series 138, National Bureau of Standards, Washington, DC; 1982.
[12] Dobry R, Pierce WG, Dyvik R, Thomas GE, Ladd RS. Pore pressure model for cyclic straining of sand [Research Report 1985-06]. Troy, NY: Rensselaer Polytechnic Institute; 1985.
[13] Green RA, Terri GA. Number of equivalent cycles concept for liquefaction evaluations—Revisited. J Geotech Geoenviron Eng 2005;131(4):477–88.
[14] Green RA, Lee J. Computation of number of equivalent strain cycles: a theoretical framework. In: Lade PV, Nakai T, editors. Geomechanics II: Testing, Modeling, and Simulation, 156. ASCE Geotechnical Special Publication; 2006. p. 471–87.
[15] Green RA, Olson SM, Cox BR, Rix GJ, Rathje E, Bachhuber J, French J, Lasley S, Martin N. Geotechnical Aspects of Failures at Port-au-Prince Seaport during the 12 January 2010 Haiti Earthquake. Earthq Spectra 2011;27(S1):S43–65.
[16] Idriss IM, Boulanger RW. Semi-empirical procedures for evaluating liquefaction potential during earthquakes. In: Proceedings of the 11th International Conference on Soil Dyn. and Earthqu, and Proceedings of the 3rd International ational Conference on Earthquake Geotech. Eng. (D. Doolin, A. Kammerer, T. Nogami, R. B. Seed, and I. Towhata, eds.), Stallion Press, Singapore;1:32–56; 2004.
[17] Idriss IM, Boulanger RW. Soil Liquefaction During Earthquakes. EERI MNO 12, Earthquake Engineering Research Institute, Oakland, CA; 2008.
[18] Ishibashi I, Zhang X. Unified dynamic shear moduli and damping ratios of sand and clay. Soils Found 1993;33(1):182–91.
[19] Jaky J. The coefficient of earth pressure at rest. Magy Mérnök és Ëpitész Egylet

Közdönye (J Soc Hung Archit Eng) 1944;78(22):355–8. [in Hungarian].
[20] Kayen R, Moss RES, Thompson EM, Seed RB, Cetin KO, Der Kiureghian A, Tanaka Y, Tokimatsu K. Shear-wave velocity–based probabilistic and deterministic assessment of seismic soil liquefaction potential. J Geotech Geoenviron Eng 2013;139(3):407–19.
[21] Lasley SJ, Green RA, Rodriguez-Marek A. New stress reduction coefficient relationship for liquefaction triggering analyses. J Geotech Geoenviron Eng 2016;142(11). [06016013-1].
[22] Lasley SJ, Green RA, Rodriguez-Marek A. Number of equivalent stress cycles for liquefaction evaluations in active tectonic and stable continental regions. J Geotech Geoenviron Eng 2017;143(4). [04016116-1].
[23] Lee J. Engineering characterization of earthquake ground motions. Ph.D. Dissertation, Department of Civil and Environmental Engineering, University of Michigan, Ann Arbor, MI; 2009.
[24] Lee J, Green RA. Number of equivalent strain cycles for active tectonic and stable continental regions. In: Proceedings 19th Intern. Conference on Soil Mechanics and Geotechnical Engineering, Seoul, Korea, 17-22 September; 2017(in press).
[25] Martin GR, Finn WDL, Seed HB. Fundamentals of liquefaction under cyclic loading. J Geotech Eng Div 1975;101(GT5):423–83.
[26] Matasovic N. [452 leaves]. Seismic response of composite horizontally-layered soil deposits xxix. Los Angeles: University of California; 1993.
[27] Matasovic N, Ordóñez GA. D-MOD2000 – a computer program for seismic site response analysis of horizontally layered soil deposits, earthfill dams, and solid waste landfills. Washington, USA: GeoMotions, LLC, Lacey; 2012.
[28] Mei X, Olson SM, Hashash YMA. Empirical curve-fitting parameters for a porewater pressure generation model for use in 1-D effective stress-based site response Analysis. 6th International Conference on Earthquake Geotechnical Engineering. Christchurch, New Zealand.
[29] Menq FY. Dynamic properties of sandy and gravelly soils. Ph.D. Dissertation, Department of Civil, Architectural, and Environmental Engineering, University of Texas, Austin, TX; 2003.
[30] Mitchell JK, Chatoian JM, Carpenter GC. The influences of sand fabric on liquefaction behavior. Report no. TE-76-1. Contract report no. S-76-5 to U.S. Army Engineer Waterways Experiment Station; 1976.
[31] Moss RES, Seed RB, Kayen RE, Stewart JP, Youd TL, Tokimatsu K. Field case histories for CPT-based in situ liquefaction potential evaluation. Geoengineering Research Report No. UCB/GE-2003/04., Univ. of California, Berkeley, CA; 2003.
[32] NRC. State of the art and practice in the assessment of earthquake-induced soil liquefaction and consequences. Washington, DC: National Research Council, The National Academies Press; 2016.
[33] Olson SM, Green RA, Lasley S, Martin N, Cox BR, Rathje E, Bachhuber J, French J. Documenting liquefaction and lateral spreading triggered by the 12 January 2010 haiti earthquake. Earthq Spectra 2011;27(S1):S93–116.
[34] Richart Jr FE, Hall JR, Woods RD. Vibrations of Soils and Foundations 401. Englewood Cliffs, New Jersey: Prentice Hall; 1970.
[35] Rodriguez-Arriaga E. Assessment of the Cyclic Strain Approach for the Evaluation of Initial Liquefaction, MS Thesis Virginia Tech, Blacksburg, VA; 2017.
[36] Silver ML, Seed HB. Volume changes in sands during cyclic loading. J Soil Mech Found Div 1971;97(SM9):1171–82.
[37] Seed HB, Idriss IM. Simplified procedure for evaluating soil liquefaction potential. J Soil Mech Found Div 1971;97(9):1249–73.
[38] Seed HB, Idriss IM, Makdisi F, Banerjee N. Representation of irregular stress time histories by equivalent uniform stress series in liquefaction analyses, EERC 75-29. Berkeley: Earthquake Engineering Research Center, University of California; 1975.
[39] Stoll RD, Kald L. Threshold of dilation under cyclic loading. J Geotech Eng Div 1977;103(GT10):1174–8.
[40] Stringer ME, Bastin S, McGann CR, Cappellaro C, El Kortbawi M, McMahon R, Wotherspoon LM, Green RA, Aricheta J, Davis R, McGlynn L, Hargraves S, van Ballegooy S, Cubrinovski M, Bradley BA, Dick G, Bellagamba X, Foster K, Lai C, Ashfield D, Baki A, Zekkos A, Lee R, Ntritsos N. Geotechnical aspects of the 2016 Kaikoura Earthquake on the South island of new Zealand. bulletin of the new Zealand Society of Earthquake engineering. 2017;50(2):117–41.
[41] Vucetic M, Dobry R. Pore pressure build-up and liquefaction at level sandy sites during earthquakes [Research Rep. CE-86-3, Dept. of Civil Engineering]. Troy, NY: Rensselaer Polytechnic Institute; 1986.
[42] Vucetic M. Cyclic threshold shear strains in soils. J Geotech Eng 1994;120:2208–28.
[43] Wair BR, Dejong JT, Shantz T. Guidelines for estimation of shear wave velocity profiles. Pacific Earthquake Engineering Research Center Report 2012/08, Pacific Earthquake Engineering Center, Berkeley, CA; 2012.
[44] Whitman RV. Resistance of soil to liquefaction and settlement. Soils Found 1971;11(4):59–68.
[45] Youd TL. Compaction of sands by repeated shear straining. J Soil Mech Found Div 1972;98(SM7):709–25.
[46] Youd TL, Idriss IM, Andrus RD, Arango I, Castro G, Christian JT, Dobry R, Finn WDL, Harder Jr LF, Hynes ME, Ishihara K, Koester JP, Liao SSC, Marcuson III WF, Martin GR, Mitchell JK, Moriwaki Y, Power MS, Robertson PK. Seed RB, Stokoe II KH. Liquefaction resistance of soils: summary report from the 1996 NCEER and 1998 NCEER/NSF workshops on evaluation of liquefaction resistance of soils. J Geotech Geoenviron Eng 2001;127(10):817–33.